ISSN 1693-4393

Catalytic Pyrolysis of Corn Cob Using Fe-Ni/Char Catalyst

Mutia Safitri[1], Muhammad Mufti Azis[1]*, Joko Wintoko[1], Jonas Kristanto[1], Novi Caroko[2]

[1]Department of Chemical Engineering, Faculty of Engineering, Universitas Gadjah Mada
[2]Department of Mechanical Engineering, Faculty of Engineering, Universitas Muhammadiyah Yogyakarta
Jl. Grafika No. 2, Sleman, Yogyakarta, Indonesia
**E-mail*: muhammad.azis@ugm.ac.id

Abstract

There is a growing interest to convert biomass waste such as corn cob to biofuel. Thermal conversion such as pyrolisis may play an important role to produce bio-oil. The objective of this research was to develop a kinetic study of catalytic pyrolysis of corn cob over Fe-Ni/Char catalyst using Thermogravimetric Analysis (TGA). The solid catalyst was prepared by impregnation method. The ratio of the percentages of Fe and Ni metals in the X-Ray Fluorescence (XRF) analysis of the catalyst was close to 1:1, resulting in metal loading values of 2.5% (1.062% and 1.013%), 5% (2.291% and 2.794%), and 10% (4.947% and 5.417%) for the catalyst. The pyrolysis experiments were performed using various catalyst loadings of 0, 2.5, 5, and 10%. In addition, the present study also investigated the influence of heating rates of 5, 10, and 20 K min^{-1}. Two isoconversion models, Kissinger-Akahira-Sunose (KAS) and Ozawa-Flynn-Wall (OFW) were utilized to determine the activation energies. The activation energies calculated using the KAS and OFW models revealed a consistent trend, with values of activation energy of corn cob pyrolysis around 124 - 303 kJ/mol and 133 - 313 kJ/mol, respectively.

***Keywords**: catalytic pyrolysis, TGA, Fe-Ni/Char catalyst, and bio-oil.*

Introduction

As the global demand for energy continues to rise, the search for sustainable, renewable energy sources has become increasingly important. The pyrolysis of biomass has emerged as a promising technology due to its potential to transform a myriad of organic waste, including agricultural residues, into valuable energy products (Bridgwater, 2012). Notably, corn cob, a common and abundant agricultural byproduct, has shown considerable promise as a feedstock for biomass pyrolysis due to its high cellulose content and low cost (Shariff et al., 2016). Improving the efficiency of corn cob pyrolysis as well as to enhance the quality of the resulting bio-oil is still challenging and one way to achieve that is by using catalysis during pyrolysis process.

In recent years, catalytic pyrolysis has been recognized for its ability to modify the distribution of pyrolysis products, improve the quality of the bio-oil, and suppress the formation of unwanted by-products (Tripathi et al., 2016). In this study, we developed a Fe-Ni/char catalyst and evaluated its efficacy in the catalytic pyrolysis of corn cob biomass. This catalyst, composed of iron and nickel supported on char, can potentially improve the bio-oil yield and its chemical composition due to its unique physicochemical properties (Sarkar & Wang, 2020). Among various catalysts, Fe-Ni/char has shown potential due to its unique physicochemical properties, including high thermal stability and excellent catalytic activity (Hu et al., 2020). Nevertheless, the application of Fe-Ni/char catalyst in the pyrolysis of corn cob biomass remains underexplored.

In the current study, we aim to address this knowledge void by undertaking a thorough kinetic analysis of corn cob pyrolysis facilitated by a Fe-Ni/char catalyst. Our focus centers on a systematic examination of the decomposition rate and the distribution of pyrolysis products, specifically exploring the impact of corn cob as a biomass feedstock and various pyrolysis conditions on the process. It is our aspiration that the insights derived from our research will enrich the overall understanding of biomass pyrolysis kinetics, thereby fostering advancements in the creation of effective and sustainable bioenergy technologies.

Previous studies from (Giudicianni et al., 2013) carried out a meticulous kinetic examination of thermal decomposition in biomass in the presence of catalysts, focusing on key constituents such as cellulose, hemicelluloses, and lignin. In another innovative approach, (Barontini et al., 2015)developed a method to study the kinetics of catalytic biomass pyrolysis using real-time evolved gas analysis in tandem with TGA, an approach that holds potential for our exploration into biomass pyrolysis. Complementing this, (Escalante et al., 2022) conducted a comparative analysis of the pyrolysis behaviors of various types of lignocellulosic biomass and algal biomass, employing catalytic Py-GC/MS and TGA. Their findings provided insights into the differential behaviors of these biomasses under pyrolytic conditions with catalysts. Furthermore, the research by (Mishra & Mohanty, 2018) into the influence of heating rate

ISSN 1693-4393

on the yield of pyrolytic products from catalyzed biomass offered valuable insights pertinent to the optimization of the pyrolysis process.

This study focuses on the utilization of the Ozawa-Flynn–Wall (OFW) and Kissinger–Akahira–Sunose (KAS) kinetic methods in examining the pyrolysis process of corncob, a widely available agricultural residue, facilitated by a Fe-Ni/Char catalyst. The FWO and KAS methods are non-isothermal techniques employed for the estimation of kinetic parameters, such as activation energy and pre-exponential factors, in complex reactions like pyrolysis. Both methods offer a simplified approach to understanding the pyrolysis process without the need for identifying or defining a kinetic mechanism.

The FWO method is a commonly used technique for analyzing the kinetics of pyrolysis reactions. It involves the analysis of the temperature-dependent conversion rate, typically obtained from Thermogravimetric Analysis (TGA) experiments. The OFW method allows for the determination of important kinetic parameters, including activation energy, pre-exponential factor, and reaction order. These parameters provide insights into the reaction mechanism and aid in process optimization. The KAS method is another widely employed approach for analyzing the kinetics of pyrolysis reactions. It utilizes the temperature dependence of the peak decomposition rate obtained from Differential Thermogravimetry (DTG). By evaluating the temperature at which the peak decomposition rate reaches a maximum, the KAS method enables the calculation of activation energy, providing valuable information about the reaction kinetics.

The primary objective of this study was to analyze the pyrolysis kinetics of corncob with Fe-Ni/Char as a catalyst, using the OFW and KAS methods. In addition, our study was aimed to enhance the comprehension of the kinetics associated with the pyrolysis process and elucidate the fundamental mechanisms in the existence of a Fe-Ni/Char catalyst. The study is expected to provide valuable insights that can aid in optimising the pyrolysis process parameters. This optimisation can lead to a more efficient conversion of corncob and other similar biomasses into biofuels and chemicals with higher value.

Materials and Methods

Materials

Corn cob powder was used as a representation of biomass that sourced from corn farmers in the Grobogan Regency of Central Java who provided the material in a coarsely chopped state. Distilled water (aquadest), a catalyst support in the form of char/activated carbon was obtained from the Coal, Gas and Petroleum Technology Lab at the Department of Chemical Engineering, UGM. Further, anhydrous $Fe(NO_3)_2{\cdot}9H_2O$ and $Ni(NO_3)_3{\cdot}6H_2O$ were obtained from Sigma-Aldrich.

Catalyst Preparation

The catalysts were prepared with three variations of Fe and Ni loadings: 2.5% with an active carbon support of 39 grams, 0.28 grams of $Fe(NO_3)_3{\cdot}9H_2O$, and 0.13 grams of $Ni(NO_3)_2{\cdot}6H_2O$. Then a 5% loading with 38 grams of active carbon, 0.62 grams of $Fe(NO_3)_3{\cdot}9H_2O$, and 0.3 grams of $Ni(NO_3)_2{\cdot}6H_2O$. Lastly, a 10% loading with 36 grams of active carbon, 1.36 grams of $Fe(NO_3)_3{\cdot}9H_2O$, and 0.76 grams of $Ni(NO_3)_2{\cdot}6H_2O$. The catalyst synthesis was initiated with calcination of the catalyst using a furnace at 500°C for 3 hours under nitrogen gas flow. Then the active carbon support was weighed according to the targeted metal loading on the catalyst. The solids $Fe(NO_3)_3{\cdot}9H_2O$ and $Ni(NO_3)_2{\cdot}6H_2O$ were also weighed based on the specified loading, then both nitrates precursors were dissolved in 100 ml of distilled water. Next, the support and metal solution were placed in a three-necked flask and stirred at a speed of 312 rpm - 318 rpm at 80°C for 4 hours. Afterwards, the sample was dried in an oven at a temperature of about 90°C - 100°C for 8 hours. Once dry, the catalyst was calcined at 500°C for 3 hours under a nitrogen gas flow. The Fe-Ni/Char catalyst was then sent to BRIN for XRF analysis to ensure the catalyst loading. BET analyses were also carried out on the char catalyst support to determine the surface area and pore size of the catalyst support.

Pyrolysis Experiments

Biomass samples, in the form of corn cobs and a mixture of biomass-catalyst, was molded into pellets with a diameter of 4 mm, a thickness of 1 mm, and a weight between 0.01 and 0.02 grams. In the mixed catalyst and biomass samples, a ratio of 1:10 was utilized. The pyrolysis process was conducted using Thermogravimetric Analysis (TGA), under a flow of nitrogen gas at a rate of 50 ml/minute, until it reaches a temperature of 500°C with three heating rate variations of approximately 5°C/minute, 10°C/minute, and 20°C/minute. This process results in a TGA curve that was subsequently used to obtain kinetic parameters through modeling.

The design of a small-scale catalytic pyrolysis system was presented in Figure 1. The apparatus commences from the carrier gas unit (N_2) and the TGA Linseis PT 1000, which functions as the site for the pyrolysis process. The samples were positioned and heated at a specific temperature within this unit. The thermogravimetric analyzer (TGA) was capable of producing a graphical representation of the temperature and time parameters associated with the pyrolysis procedure.

ISSN 1693-4393

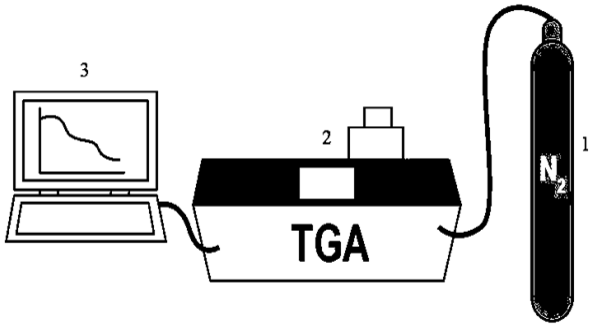

Keterangan:

1. Nitrogen Gas Cylinder Tank
2. TGA Linesis PT 1000
3. Computer

Figure 1. Schematic diagram of Thermogravimetric Analysis (TGA)

Kinetic Modeling Method

According to Vyazovkin et al. (2011), the general process of pyrolysis can be described as follows:

Biomass ⟶ Char + Volatile + Gas

The kinetic method that is widely applied to thermal analysis uses the reaction rate as a function of two variables, namely T (temperature) and α (conversion) as the following equation:

$$\frac{d\alpha}{dt} = k(T)f(\alpha) \quad (1)$$

The reaction rate constant is expressed by the Arrhenius equation:

$$k(T) = Aexp\left(\frac{-E}{RT}\right) \quad (2)$$

By substituting equation (2) into equation (1), the following is obtained

$$\frac{d\alpha}{dt} = Aexp\left(\frac{-E}{RT}\right)f(\alpha) \quad (3)$$

In equation (3), if f(α) is used to describe the first-order solid-state reaction, then the function f(α) becomes:

$$f(\alpha) = (1-\alpha)^n \quad (4)$$

where n = reaction order

The next step is to substitute equation (4) into equation (3) to obtain the following equation:

$$\frac{d\alpha}{dt} = A(1-\alpha)^n exp\left(\frac{-E}{RT}\right) \quad (5)$$

In general, the non-isothermal process will experience a linear change in temperature over time as follows:

$$\beta = \frac{dT}{dt} \quad (6)$$

where β = heating rate, thus equation (4) can be rearranged to:

$$dt = \frac{\beta}{dT} \quad (7)$$

Substitute equation (7) into equation (5) to obtain the following equation:

$$\frac{d\alpha}{dT} = \frac{A}{\beta}(1-\alpha)^n exp\left(\frac{-E}{RT}\right) \quad (8)$$

Therefore, equations (8) and (5) can be stated as the fundamental analysis method to determine kinetic parameters based on TGA (Thermogravimetric Analysis) data.

The determination of kinetic parameters was accomplished using various curves, each of which was characterized by differing heating rates yet identical feedstock conversion levels. The International Confederation for Thermal Analysis and Calorimetry (ICTAC) Kinetics Committee endorses these processes. Several methods, including Vyazovkin (V), Kissinger–Friedman (FR), Ozawa-Flynn–Wall (OFW), and Kissinger–Akahira–Sunose (KAS), have been recognized as superior practices for isoconversional methods. In this study, two distinct methods, namely KAS and OFW, were utilized. Both methods were additionally employed to estimate the apparent activation energy.

The corresponding equations are elaborated as follows:

For the Kissinger–Akahira–Sunose (KAS) method, the equation is given as:

ISSN 1693-4393

$$ln\left(\frac{\beta}{T^2}\right) = ln\left(\frac{AE}{R \cdot g(\alpha)}\right) - \left(\frac{E}{RT}\right) \quad (9)$$

The apparent activation energy can be retrieved from a plot of ln(β/T) vs. 1/T for a given value of conversion α, where the slope = -E/R.

For the Flynn–Wall–Ozawa (FWO) method, the equation is:

$$ln(\beta) = ln\left(\frac{AE}{E \cdot g(\alpha)}\right) - 5.331 - 1.052\left(\frac{E}{RT}\right) \quad (10)$$

Where, 1/T = the linear relation with a given value of conversion at various heating rates and α = given value of conversion, respectively. The activation energy Eα was estimated from the slope -1.052E/R.

Where,
β = represents the heating rate
T = signifies the temperature
R = denotes the gas constant (8.314 J/K mol)
A = is the pre-exponential factor (s^{-1})
E = is the activation energy (kJ/mol)
g(α) = is a constant at a known conversion value

Results and Discussion

Catalyst characterization

The catalyst used in this research is a bimetal catalyst with char support, which was impregnated with a solution of Fe and Ni metals. The char catalyst support produced a type IV hysteresis loop (Xu et al., 2020), which indicates that the char is a mesoporous material with a diameter size ranging from 2 nm to 50 nm and possesses narrow slit-shaped pores. Further data obtained shows a BET surface area of 200.836 m^2/g, a total pore volume of 0.346 cm^3/g, and an average pore diameter of 2.001 nm.

The metals used are in the form of anhydrous with the chemical formula $Fe(NO_3)_3 \cdot 9H_2O$ and $Ni(NO_3)_3 \cdot 6H_2O$. The catalyst was made in several loading variations, 0%, 2.5%, 5%, and 10% with the ratio of Fe and Ni metal percentages being 1:1. To determine whether the metal loading percentage in the catalyst was appropriate, an XRF (X-ray fluorescence) test was performed. The results of the XRF test on the catalyst can be seen in table 1.

Table 1. Percentage of Fe-Ni/Char Catalyst loading in XRF

Element	Chemical Composition (%)		
	Fe-Ni/Char 2,5%	Fe-Ni/Char 5%	Fe-Ni/Char 10%
Fe	1.062	2.291	4.947
Ni	1.013	2.794	5.417

The data obtained from the XRF test indicated that the percentage of Fe and Ni loading was almost close to the desired percentage after impregnating the catalyst three times.

Thermogravimetry Analysis (TGA)

The thermal testing was conducted on corn cob powder samples using a Thermogravimetric Analysis (TGA) instrument, resulting in a decomposition profile of the biomass and catalyst samples against temperature. The obtained data were processed into a TGA curve which was used as the main raw material for the analysis of the pyrolysis process. The TGA curve can explain the process of sample mass changes in response to temperature increases at various phase change stages. The pyrolysis process of corn cob biomass will be carried out with several variations of Fe-Ni/Char loading catalysts which can be seen in Figure 2 with heating rates of 5, 10, and 20 °C/minute.

According to (Mishra & Mohanty, 2018), there are three main phases in the pyrolysis process on the TGA curve: the drying phase which occurs at temperatures less than 150-200°C, the devolatilization phase at temperatures 200-500°C, and the char formation phase at temperatures above 500°C. The drying phase involves the process of reducing the water content in the sample, which often also includes compounds with relatively low molecular weights. The other two phases are the active pyrolysis zones where the decomposition of the corn cob powder occurs as the core process, so it is known that the active pyrolysis zone begins to take place after the drying process ends. The explanation by Foong et al. (2020) also supports the previous opinion that the drying process of the sample occurs below 150°C, hence data fluctuation occurs. Therefore, the TGA curve will start from temperatures of 150°C up to 600°C, where this temperature range is the active pyrolysis zone that will show the profile of the biomass decomposition process.

ISSN 1693-4393

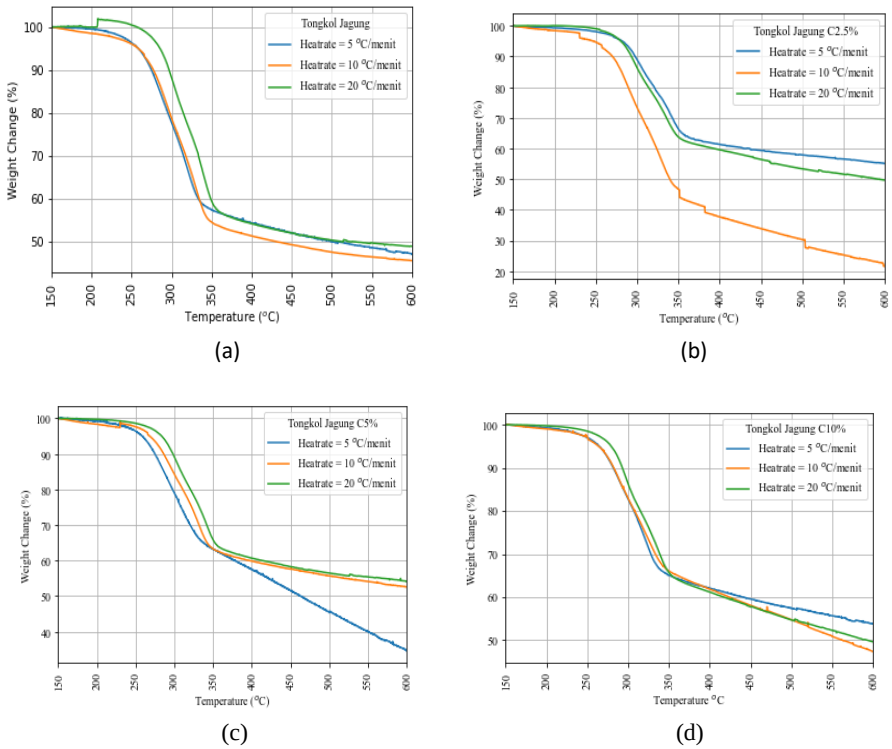

Figure 2. TGA curve (a) Corn Cob 0% Catalyst, (b) Corn Cob 2.5% Catalyst, (c) Corn Cob 5% Catalyst, and (d) Corn Cob 10% Catalyst

Based on Figure 2, the pyrolysis process with TGA was performed at three different heating rates. In Figure 2 (a), the curve displays the result of pyrolysis of corn cobs without a catalyst, where three different heating rates are evident. The decomposition process of the sample at 600˚C results in the least amount of residue at a heating rate of 10˚C/minute, around 44%, while the heating rates of 5˚C/minute and 20˚C/minute each produced residues around 46% and 49% respectively. The obtained results from the corn cob pyrolysis indicate the influence of heating rate on the sample conversion process, hence resulting in different residues at each heating rate. A study by (Wang et al., 2018) also discovered that varying heating rates in biomass pyrolysis yield varying residues, where lower heating rates generate less residue compared to higher heating rates at a certain temperature.

Figure 2 (b) represents the TGA curve of the pyrolysis sample mixture of corn cobs and Fe-Ni/Char 2.5% catalyst. The noticeable mass reduction process occurs significantly in the temperature range of 200-300˚C. The curve shows that the least amount of residue at 600˚C is obtained at a heating rate of 10˚C/minute, around 23%, while at heating rates of 5˚C/minute and 20˚C/minute, residues of around 55% and 50% are obtained, respectively. This result suggests that corn cob pyrolysis with the addition of 2.5% Fe-Ni/Char catalyst works more effectively at a heating rate of 10˚C/minute. A study by (Hu et al., 2020) reported that the addition of Fe-Ni/Char catalyst to corn cob pyrolysis can enhance the efficiency of the pyrolysis process, thereby increasing the yield of the produced product.

The addition of 5% Fe-Ni/Char catalyst to corn cob pyrolysis resulted in the TGA curve shown in Figure 2 (c), where a heating rate of 5˚C/minute produces the least residue, about 34%, while heating rates of 10˚C/minute and 20˚C/minute result in residues of about 52% and 54%. Thus, a heating rate of 5˚C/minute is a suitable condition for using a 5% catalyst loading in this pyrolysis process. Figure 2 (d) shows the TGA curve of the pyrolysis process of corn cobs with the addition of 10% Fe-Ni/Char catalyst. The curve shows that the least residue from the pyrolysis process is obtained at a heating rate of 10˚C/minute, around 45%, while residues of about 53% and 49% are obtained at heating rates of 5˚C/minute and 20˚C/minute, respectively.

Based on the results obtained from the TGA curve with catalyst loading variations of 0%, 2.5%, 5%, and 10%, it is found that the 2.5% Fe-Ni/Char catalyst at a heating rate of 10˚C/minute effectively influences the decomposition of corn cob biomass, as seen in the least residue produced. This indicates that these conditions are the best for the decomposition process of corn cob biomass. In a previous study by (Liang et al., 2020), the effect of catalyst loading variations.

The devolatilization process in each TGA curve in Figure 2 starts at a temperature of around 220°C and progresses rapidly with increasing temperature up to 340-360°C. However, after this, the trend of sample mass reduction occurs gradually until the final temperature. A study by (Barontini et al., 2015) observed the devolatilization process in

ISSN 1693-4393

pyrolysis of several types of biomass using TGA analysis. The results obtained showed that devolatilization starts at a relatively low temperature and proceeds quickly up to a certain temperature, followed by a slower mass reduction.

Derivative Thermogravimetry (DTG)

DTG analysis is necessary to explain TGA as it provides more detailed information about the thermal properties of the sample. TGA measures the mass decrease of the material when heated, while DTG shows the rate of mass decrease at different temperatures. DTG is also useful for observing mass changes that are not easily visible on the TGA thermogram (Xing et al., 2014). DTG can also demonstrate the mechanism by which material loses mass from controlled heating (Liu et al., 2014).

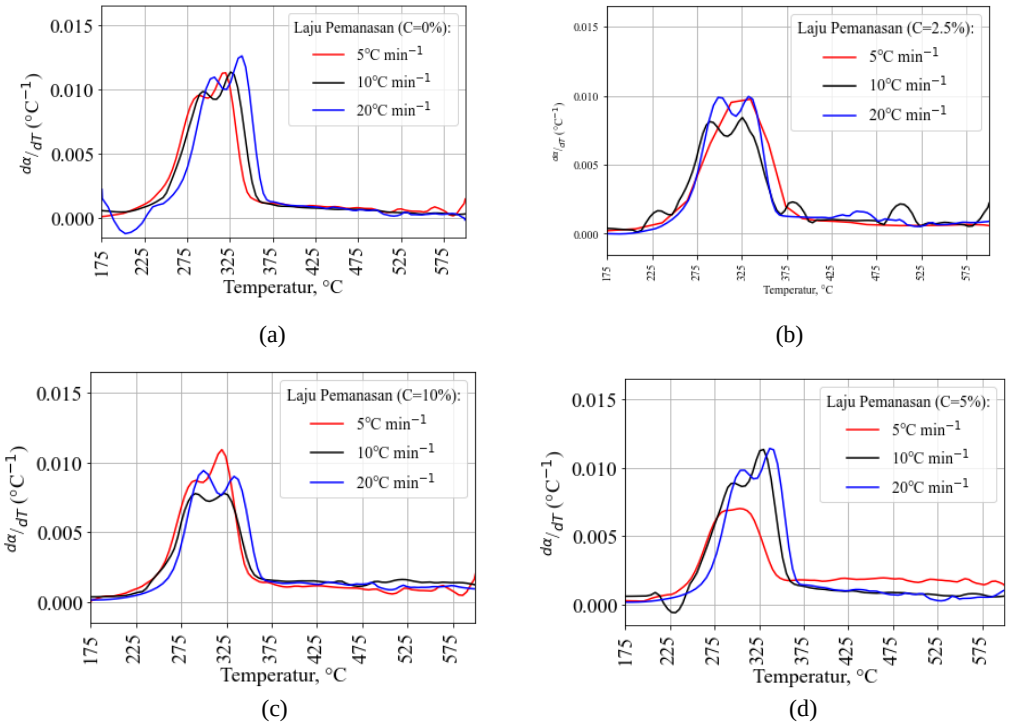

Figure 1 DTG curve (a) Corn Cob 0% Catalyst, (b) Corn Cob 2.5% Catalyst, (c) Corn Cob 5% Catalyst, and (d) Corn Cob 10% Catalyst

Based on the characterization from the TGA and DTG thermograms from Figure 2 (a-d) and Figure 3 (a-d), the pyrolysis reaction of corn cob biomass can be divided into two stages. The first stage starts at a temperature of 230 - 380°C, where there is a significant mass loss. Subsequently, the second stage starts from temperatures above 380°C up to the final pyrolysis temperature (600°C), where the mass change tends to be less significant compared to the first stage. The decomposition of hemicellulose and cellulose generally occurs in the first stage with a temperature range of 230 - 380°C. Meanwhile, the decomposition of lignin occurs in a wider temperature range, starting from temperatures below 230 - 380°C up to the final pyrolysis temperature. The temperature range of decomposition of this sample is already in accordance with previous research conducted by (Minh Loy et al., 2018).

Furthermore, the devolatilization of hemicellulose and cellulose occurs at temperatures between 255 and 380°C, and the breakdown of lignin takes place between 650 and 900°C. Referring to (Yang et al., 2007), hemicellulose contains many compounds with C=O bonds that decompose in the temperature range 200-314°C, while cellulose contains two strong -OH and C-O functional groups, which decompose in the temperature range 314-409°C. Lignin decomposes over a wider temperature range because it has very strong bonds in the aromatic ring structure (examples: phenol and benzene). Lignin is rich in O-CH_3, C-O-C, and C=C bonds, requiring a wide temperature range to decompose fully. In addition, hemicellulose and lignin contribute to the amount of residue produced; both leave solid residues even when pyrolyzed at high temperatures.

ISSN 1693-4393

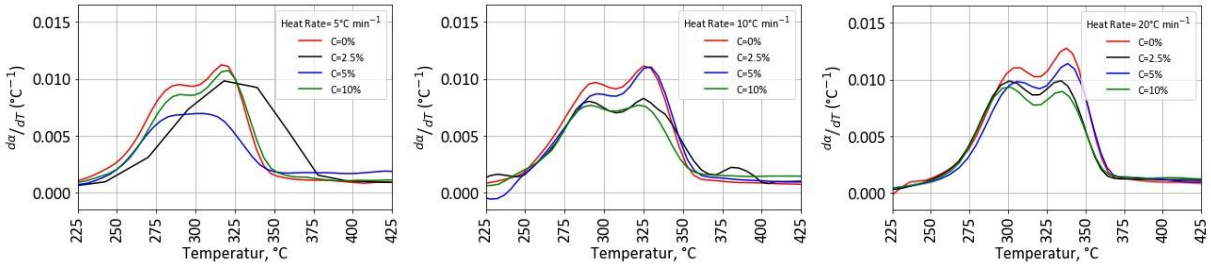

(a) (b) (c)

Figure 4. DTG Curve (a) Heatrate 5˚C/minute (b) Heatrate 10˚C/minute (c) Heatrate 20˚C/minute

To further study the influence of heat rate and catalyst, the curve is modified to display the behavior of different catalyst concentrations at different heat rates. In the observed DTG curve, generally one type of reaction variable has a peak splitting, as shown in Figure 3 (a) and (c) for all heat rates. Meanwhile, reactions without peak splitting are shown in Figure 3 (b) and (d) for a heat rate of 5°C/minute. Mulokozi et al. (2018) argue that peak splitting is a phenomenon that occurs at high heat rates. Because high heat rates tend to separate thermal decomposition into two kinetic phases. This also indicates that the decomposition process occurs in several stages or steps, not just one.

Figures 3 (a-d) and Figure 4 (a-c) also show the value of the peak getting higher at higher heat rates. This trend is also similar to other studies such as the research by (Minh Loy et al., 2018), and (Lim et al., 2012). Except at a catalyst concentration of 10%, where the highest observed peak is seen at a heat rate of 5°C/minute. Meanwhile, Figure 4 shows that the highest peak is always obtained by Pyrolysis without a catalyst, (Kim et al., 2018) found that the pyrolysis of P. densiflora also experiences the same thing. This is caused by the formation of coke on the outer surface and pores of the catalyst.

Furthermore, based on the TGA curve, it is found that at a catalyst concentration of 2.5% and a heat rate of 10°C/minute, the least residue value is obtained around 30%. After observing through the DTG curve Figure 2 (c), it is found that there is a peak above the temperature of the first stage. This means that there is a significant second stage reaction, marked by the appearance of several lower peaks, this is most likely because at that concentration and heat rate, lignin begins to decompose, resulting in a reduction in the residue from that reaction.

Kinetic Study

The data analysis obtained from TGA using the isoconversional model, namely KAS and OFW in this study, both numerical calculations and kinetic parameter estimation were conducted in the Python programming language on Spyder (Python IDE) which can be seen in figure 5. and table 2.

During the conversion of biomass to bioenergy, a significant criterion, namely kinetic analysis, becomes the basis for the creation of an optimal thermochemical process design (Kaur et al., 2018). The thermogravimetric analysis performed is then interpreted with the KAS and OFW methods to calculate kinetic parameters with different catalyst loadings. The fractional conversion range is narrowed from 0.1 to 0.8 to observe the difference in activation energy values during the thermal decomposition process and to avoid a rather extreme decrease in activation energy.

Activation energy can be defined as the minimum energy required to trigger a reaction process. However, triggering a reaction that requires a high activation energy poses its own challenge. Changes in activation energy are illustrated in Figures 5 (a) dan (c) there is an increase in activation energy (E), indicating the presence of an endothermic reaction marked by an increase in activation energy from conversion 0.1 to 0.4 and conversion 0.1 to 0.8. While Figures 5 (b) and (d) increase in activation energy continues to occur until conversion 0.8.

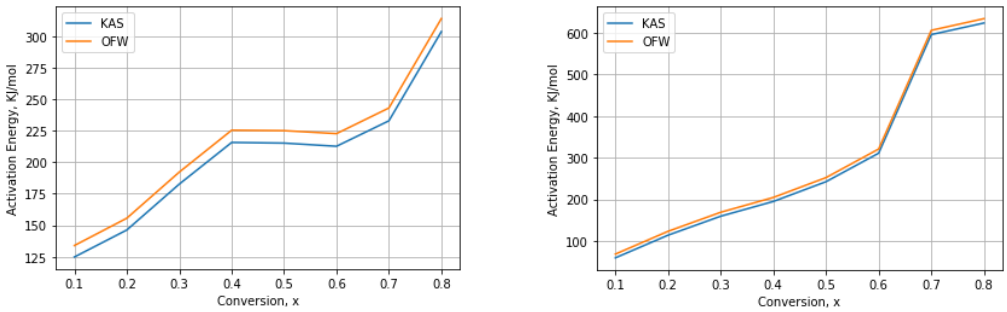

(a) (b)

ISSN 1693-4393

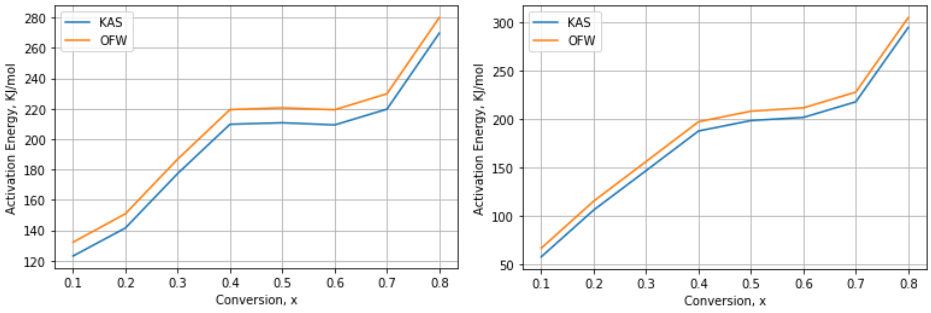

(c) (d)

Figure 4. KAS and OFW Trend of (a) Corn Cob 0% Catalyst, (b) Corn Cob 2.5% Catalyst, (c) Corn Cob 5% Catalyst, and (d) Corn Cob 10% Catalyst

Table 2. The Activation Energy Value from the Application of KAS and FWO Models

Components	α	KAS			FWO		
		Equation	R^2	E (kJ/mol)	Equation	R^2	E (kJ/mol)
Corn Cob 0% Fe-Ni/Char	0,1	y = 17.44 +-15007.95x	0.9951	124.7760	y = 32.05 +-16103.36x	0.9957	133.8833
	0,2	y = 21.23 +-17586.82x	0.9965	146.2168	y = 35.90 +-18712.30x	0.9969	155.5740
	0,3	y = 28.26 +-21962.83x	0.9985	182.5989	y = 42.97 +-23109.17x	0.9986	192.1296
	0,4	y = 34.38 +-25940.58x	0.9971	215.6699	y = 49.11 +-27107.37x	0.9973	225.370
	0,5	y = 33.44 +-25878.94x	0.9980	215.15753	y = 48.21 +-27067.11x	0.9982	225.0359
	0.6	y = 32.23 +-25575.97x	0.9989	212.6385	y = 47.04 +-26782.69x	0.9990	222.6713
	0.7	y = 35.61 +-28008.55x	0.9991	232.8631	y = 50.44 +-29231.77x	0.9992	243.0329
	0.8	y = 48.52 +-36519.19x	0.9930	303.6205	y = 63.38 +-37762.72x	0.9934	313.9592
Corn Cob 2.5% Fe-Ni/Char	0,1	y = 3.25 +-7132.46x	0.9918	59.2992	y = 17.84 +-8213.76x	0.9938	68.2891
	0,2	y = 14.51 +-13679.67x	0.9982	113.7327	y = 29.16 +-14796.09x	0.9985	123.0146
	0,3	y = 23.66 +-19163.19x	0.9985	159.3227	y = 38.35 +-20300.47x	0.9987	168.7781
	0,4	y = 30.36 +-23428.12x	0.9975	194.7813	y = 45.09 +-24586.84x	0.9978	204.4149
	0,5	y = 39.16 +-29137.35x	0.9956	242.2479	y = 53.93 +-30319.92x	0.9959	252.0797
	0.6	y = 51.94 +-37378.34x	0.9963	310.7635	y = 66.74 +-38582.37x	0.9965	320.7738
	0.7	y = 106.85 +-71669.70x	0.9836	595.8618	y = 121.69 +-72894.35x	0.9841	606.0435
	0.8	y = 109.01 +-75015.50x	0.8663	623.6788	y = 123.90 +-76273.76x	0.8701	634.1400
Corn Cob 5% Fe-Ni/Char	0,1	y = 17.10 +-14798.19x	0.9952	123.0321	y = 31.71 +-15891.76x	0.9959	132.1241
	0.2	y = 20.28 +-17019.00x	0.9964	141.4959	y = 34.94 +-18142.51x	0.9968	150.8368
	0,3	y = 27.26 +-21333.88x	0.9983	177.3698	y = 41.96 +-22477.60x	0.9985	186.8788
	0,4	y = 33.31 +-25232.95x	0.9982	209.7867	y = 48.04 +-26395.89x	0.9984	219.4554
	0.5	y = 32.71 +-25351.86x	0.9983	210.7753	y = 47.48 +-26535.70x	0.9985	220.6178
	0,6	y = 31.75 +-25181.19x	0.9991	206.3564	y = 46.54 +-26383.33x	0.9992	219.3510
	0,7	y = 33.22 +-26428.60x	0.9994	219.7274	y = 48.04 +-27646.69x	0.9994	229.8545
	0.8	y = 42.34 +-32446.82x	0.9978	269.7628	y = 57.19 +-33682.00x	0.9979	280.0321
Corn Cob 10% Fe-Ni/Char	0,1	y = 3.11 +-6943.22x	0.9941	57.7260	y = 17.66 +-8010.19x	0.9956	66.5967
	0,2	y = 13.06 +-12744.38x	0.9966	105.9568	y = 27.69 +-13850.58x	0.9972	115.1538
	0,3	y = 21.29 +-17632.05x	0.9978	146.5928	y = 35.96 +-18758.35x	0.9980	155.9569
	0,4	y = 29.38 +-22544.92x	0.9982	187.4385	y = 44.08 +-23688.53x	0.9984	196.9464
	0,5	y = 30.90 +-23840.15x	0.9974	198.2070	y = 45.64 +-25003.47x	0.9977	207.8788
	0.6	y = 30.81 +-24228.84x	0.9980	201.4386	y = 45.57 +-25412.90x	0.9982	211.2829
	0.7	y = 33.34 +-26162.13x	0.9984	217.5120	y = 48.14 +-27365.18x	0.9986	227.5141
	0.8	y = 47.75 +-35379.08x	0.9953	294.1417	y = 62.58 +-36600.53x	0.9957	304.2968

ISSN 1693-4393

In Table 2, it can be observed that the minimum activation energy value for corn cob is present at the addition of 2.5% and 10% catalysts, which is around 66 and 68 kJ/mol. This value is comparable with another finding on the pyrolysis of corn cobs conducted by (Arenas Castiblanco et al., 2022) that the activation energy varied between 60 to 70 kJ/mol at the end of the pyrolysis experiment.

The activation energies obtained from the FWO and KAS methods tend to increase as the conversion value increases. For the KAS method, the activation energy increased from 133 to 313 kJ/mol in the pyrolysis of corn cob without a catalyst. Then, the activation energy in the pyrolysis of corn cob with the addition of 5% and 10% catalysts also showed an increase in activation energy starting from 66 to 304 kJ/mol for 10% catalyst, and 132 to 280 kJ/mol for 5% catalyst. Meanwhile, the pyrolysis of corn cob with the addition of 2.5% catalyst obtained quite a large activation energy at conversion 0.8, which is about 634 kJ/mol. The results of the kinetic analysis revealed that the activation energy is highly dependent on the conversion of biomass. When the conversion process proceeds, the variations in the reaction mechanism were clearly noticed which caused a significant variation in the activation energy values (Table 4). The higher activation energy values represent a comparatively reluctant reaction since the activation energy is the minimum energy required to initiate a reaction process. Moreover, to calculate the reactivity of a fuel, the knowledge of E will also be helpful (Gai et al., 2013).

A study by (Sarkar & Wang, 2020) examining the pyrolysis kinetics of jute stems stated that the obtained activation energy increased from 119.90 to 148.12 kJ/mol, and after this, it was reduced to 140.71 kJ/mol in the FWO method. On the other hand, for the KAS method, it increased from 116.70 to 144.95 kJ/mol and then decreased to 136.86 kJ/mol, respectively. In addition, in this paper, the calculated activation energy values for jute stick were found to be consistent with previous research. This is comparable to the activation energy obtained in the pyrolysis process of corn cob with variations of 0%, 5%, and 10% catalysts. However, at the addition of 2.5% catalyst for conversions 0.7 and 0.8, the activation energy increased significantly, which may indicate that the processes involved are more complex and involve different reaction mechanisms or stages, or that the reaction conditions are quite extreme.

Conclusion

Kinetic modeling was performed on the pyrolysis of corn cobs with the addition of catalysts in various loadings of 2.5%, 5%, and 10% using an isoconversional approach. The kinetic analysis results applying the KAS and OFW methods for all samples provided nearly similar trends. In the pyrolysis of corn cobs, the activation energy decreased only at the conversion of 0.4 to 0.6 for corn cobs with 0% and 5% catalyst loading, ranging between 215-212kJ/mol and 209-206kJ/mol, respectively. For corn cobs with the addition of 2.5% and 10% catalyst loading, the activation energy tended to increase with the increase in conversion, with activation energy ranges between 59-623kJ/mol and 57-294kJ/mol, respectively. The pyrolysis of corn cobs with catalyst loadings of 0%, 5%, and 10% yielded quite good results using the KAS and OFW methods where the resulting activation energy was quite stable and there was a decrease in activation energy at a certain conversion level. However, at 2.5% catalyst, the resulting activation energy was very large, thus further kinetic analysis is needed for the multistage nature of the pyrolysis reaction.

Acknowledgments

We would like to thank the partial financial support from the research grant of Department of Chemical Engineering UGM in this work. We would also like to thank Mr. Pandu Satya Permana for his practical help in the analyses of our samples.

References

Arenas Castiblanco, E., Montoya, J. H., Rincón, G. V., Zapata-Benabithe, Z., Gómez-Vásquez, R., & Camargo-Trillos, D. A. (2022). A new approach to obtain kinetic parameters of corn cob pyrolysis catalyzed with CaO and CaCO3. *Heliyon*, *8*(8). https://doi.org/10.1016/j.heliyon.2022.e10195

Barontini, F., Biagini, E., Bonini, F., & Tognotti, L. (2015). An experimental investigation on the devolatilization behaviour of raw and torrefied lignocellulosic biofuels. *Chemical Engineering Transactions*, *43*, 481–486. https://doi.org/10.3303/CET1543081

Bridgwater, A. V. (2012). Review of fast pyrolysis of biomass and product upgrading. *Biomass and Bioenergy*, *38*, 68–94. https://doi.org/10.1016/j.biombioe.2011.01.048

Escalante, J., Chen, W. H., Tabatabaei, M., Hoang, A. T., Kwon, E. E., Andrew Lin, K. Y., & Saravanakumar, A. (2022). Pyrolysis of lignocellulosic, algal, plastic, and other biomass wastes for biofuel production and circular bioeconomy: A review of thermogravimetric analysis (TGA) approach. *Renewable and Sustainable Energy Reviews*, *169*(May), 112914. https://doi.org/10.1016/j.rser.2022.112914

Gai, C., Dong, Y., & Zhang, T. (2013). The kinetic analysis of the pyrolysis of agricultural residue under non-isothermal conditions. *Bioresource Technology*, *127*, 298–305. https://doi.org/10.1016/j.biortech.2012.09.089

Giudicianni, P., Cardone, G., & Ragucci, R. (2013). Cellulose, hemicellulose and lignin slow steam pyrolysis: Thermal decomposition of biomass components mixtures. *Journal of Analytical and Applied Pyrolysis*, *100*, 213–222. https://doi.org/10.1016/j.jaap.2012.12.026

ISSN 1693-4393

Hu, M., Cui, B., Xiao, B., Luo, S., & Guo, D. (2020). Insight into the ex situ catalytic pyrolysis of biomass over char supported metals catalyst: Syngas production and tar decomposition. *Nanomaterials*, *10*(7), 1–14. https://doi.org/10.3390/nano10071397

Kaur, R., Gera, P., Jha, M. K., & Bhaskar, T. (2018). Pyrolysis kinetics and thermodynamic parameters of castor (Ricinus communis) residue using thermogravimetric analysis. *Bioresource Technology*, *250*, 422–428. https://doi.org/10.1016/j.biortech.2017.11.077

Kim, Y.-M., Rhee, G. H., Ko, C. H., Kim, K. H., Jung, K. Y., Kim, J. M., & Park, Y.-K. (2018). Catalytic Pyrolysis of Pinus densiflora Over Mesoporous Al 2 O 3 Catalysts . *Journal of Nanoscience and Nanotechnology*, *18*(9), 6300–6303. https://doi.org/10.1166/jnn.2018.15653

Liang, S., Guo, F., Du, S., Tian, B., Dong, Y., Jia, X., & Qian, L. (2020). Synthesis of Sargassum char-supported Ni-Fe nanoparticles and its application in tar cracking during biomass pyrolysis. *Fuel*, *275*(January), 117923. https://doi.org/10.1016/j.fuel.2020.117923

Lim, J. S., Abdul Manan, Z., Wan Alwi, S. R., & Hashim, H. (2012). A review on utilisation of biomass from rice industry as a source of renewable energy. *Renewable and Sustainable Energy Reviews*, *16*(5), 3084–3094. https://doi.org/10.1016/j.rser.2012.02.051

Liu, X., Xia, W., Jiang, Q., Xu, Y., & Yu, P. (2014). Synthesis, characterization, and antimicrobial activity of kojic acid grafted chitosan oligosaccharide. *Journal of Agricultural and Food Chemistry*, *62*(1), 297–303. https://doi.org/10.1021/jf404026f

Minh Loy, A. C., Yusup, S., Fui Chin, B. L., Wai Gan, D. K., Shahbaz, M., Acda, M. N., Unrean, P., & Rianawati, E. (2018). Comparative study of in-situ catalytic pyrolysis of rice husk for syngas production: Kinetics modelling and product gas analysis. *Journal of Cleaner Production*, *197*, 1231–1243. https://doi.org/10.1016/j.jclepro.2018.06.245

Mishra, R. K., & Mohanty, K. (2018). Pyrolysis kinetics and thermal behavior of waste sawdust biomass using thermogravimetric analysis. *Bioresource Technology*, *251*, 63–74. https://doi.org/10.1016/j.biortech.2017.12.029

Sarkar, J. K., & Wang, Q. (2020). Characterization of pyrolysis products and kinetic analysis of waste jute stick biomass. *Processes*, *8*(7). https://doi.org/10.3390/pr8070837

Shariff, A., Aziz, N. S. M., Ismail, N. I., & Abdullah, N. (2016). Corn cob as a potential feedstock for slow pyrolysis of biomass. *Journal of Physical Science*, *27*(2), 123–137. https://doi.org/10.21315/jps2016.27.2.9

Tripathi, M., Sahu, J. N., & Ganesan, P. (2016). Effect of process parameters on production of biochar from biomass waste through pyrolysis: A review. *Renewable and Sustainable Energy Reviews*, *55*, 467–481. https://doi.org/10.1016/j.rser.2015.10.122

Wang, Y. J., Kang, K., Yao, Z. L., Sun, G. T., Qiu, L., Zhao, L. X., & Wang, G. (2018). Effects of different heating patterns on the decomposition behavior of white pine wood during slow pyrolysis. *International Journal of Agricultural and Biological Engineering*, *11*(5), 218–223. https://doi.org/10.25165/j.ijabe.20181105.3156

Xing, R., Guo, J., Miao, C., Liu, S., & Pan, H. (2014). Fabrication of protein-coated CdS nanocrystals via microwave-assisted hydrothermal method. *Journal of Experimental Nanoscience*, *9*(6), 582–587. https://doi.org/10.1080/17458080.2012.678891

Xu, L., Zhang, J., Ding, J., Liu, T., Shi, G., Li, X., Dang, W., Cheng, Y., & Guo, R. (2020). Pore structure and fractal characteristics of different shale lithofacies in the dalong formation in the western area of the lower yangtze platform. *Minerals*, *10*(1). https://doi.org/10.3390/min10010072

Yang, H., Yan, R., Chen, H., Lee, D. H., & Zheng, C. (2007). Characteristics of hemicellulose, cellulose and lignin pyrolysis. *Fuel*, *86*(12–13), 1781–1788. https://doi.org/10.1016/j.fuel.2006.12.013